Journal of Alloys and Compounds 507 (2010) 331–334

Contents lists available at ScienceDirect

Journal of Alloys and Compounds

journal homepage: www.elsevier.com/locate/jallcom

Estimation of driving force for martensitic transformation in $(Ni_{52.5}Mn_{23.5}Ga_{24})_{100-x}Co_x$ alloys

Shaomeng Yan, Jian Pu, Bo Chi, Li Jian*

School of Materials Science and Engineering, State Key Laboratory of Material Processing and Die & Mould Technology, Huazhong University of Science & Technology, 1037 Luo Yu Road, Wuhan, Hubei 430074, China

ARTICLE INFO

Article history:
Received 22 April 2010
Received in revised form 26 July 2010
Accepted 27 July 2010
Available online 4 August 2010

Keywords:
Ni_2MnGa
Martensitic phase transformation
Driving force
Yield strength
Shape deformation

ABSTRACT

$(Ni_{52.5}Mn_{23.5}Ga_{24})_{100-x}Co_x$ (x = 2, 4, 6, 8) alloys were prepared for the determination of their characteristic phase transformation temperatures (M_s, M_f, A_s, A_f) and high temperature yield strength of the parent phase. The driving force for the martensitic phase transformation in these alloys was estimated from thermodynamic point of view by taking into account the contributions of the shape deformation and the twin formation accompanying the martensitic phase transformation to the energy required to initiate the transformation; and a positive linear relationship between the driving force and the yield strength of the parent phase at M_s temperature was established.

1. Introduction

Ferromagnetic shape memory alloys (FSMAs) that simultaneously show shape memory effect (SME) and ferromagnetic behavior have attracted great attention due to their potential applications as smart materials [1,2]. The most interesting member of the FSMAs is the Heusler alloy, known as a group of ternary intermetallic compounds with a stoichiometric composition of Ni_2MnGa, which is found to produce a significant strain under the bias of a magnetic field [1,3–5] and exhibits thermally and magnetically driven SME with a rapid and efficient response. This property of the Ni–Mn–Ga alloy is associated with the martensitic transformation from the parent phase to the martensitic phase upon cooling and the magnetic field-induced motion of twin boundaries. This is different from the mechanism responsible for the large strain in conventional thermal shape memory alloys.

In Ni_2MnGa system, the parent phase has a cubic $L2_1$ structure with a space group $Fm3m$, whereas the structure of the martensitic phase can be 5-layer modulated (5M), 7-layer modulated (7M) or non-modulated (NM) depending on the composition of the alloy [6,7]. Several studies have suggested that the starting temperature of martensite transformation (M_s) is a function of the valence electron concentration (e/a) and/or the volume of the unit cell of the alloy [8–10]. Heat treatment also alters the M_s via the ordering of the $L2_1$ phase in a small scale [11,12]. These conclusions have also been confirmed in Ni–Fe–Ga alloys and the Ge-, Co- or Fe-added Ni–Mn–Ga alloys [13–15].

As well known, martensitic transformation is a diffusionless transformation in which shape deformation is a major step to form the final structure of the martensite. Therefore, the yield strength of the parent phase at the transformation temperature, usually the $\sigma_{0.2}(M_s)$, has also been considered a major resistance to the martensitic transformation [16], which acts as a part of the non-chemical free energy of the transformation and determines the M_s temperature. The purpose of the present study is to establish a relationship between the $\sigma_{0.2}(M_s)$ and the driving force of martensitic transformation in Co-added Ni_2MnGa alloys from the point of view of thermodynamics.

2. Experimental

Four polycrystalline ingots of $(Ni_{52.5}Mn_{23.5}Ga_{24})_{100-x}Co_x$ (x = 2, 4, 6, 8) alloys, designated as C2, C4, C6 and C8, respectively, in order to specify the amount of Co added, were prepared by arc melting in argon atmosphere with appropriate amounts of Ni, Mn, Ga and Co at a purity of 99.95 wt.%. Each ingot was repeatedly melted in a water-cooled copper crucible for five times to ensure compositional homogeneity. Afterwards, the melted alloy was suck-cast into a water-cooled cylindrical copper mold placed at the bottom of the arc furnace to form an alloy rod with a constant diameter of 5 mm. The alloy rods were annealed in evacuated quartz tubes at 1000 °C for 48 h for further homogenization. Chemical compositions of the alloys were analyzed using an X-ray fluorescence spectroscope (XRF, EAGLE III), as listed in Table 1. The analyzed composition was somewhat deviated from the designed composition due to element volatilization, especially Mn, during alloy preparation and homogenization.

* Corresponding author. Tel.: +86 27 87557694; fax: +86 27 87558142.
E-mail address: lijian@hust.edu.cn (L. Jian).

0925-8388/$ – see front matter © 2010 Elsevier B.V. All rights reserved.
doi:10.1016/j.jallcom.2010.07.194

Table 1
Chemical composition of prepared alloys determined by XRF in comparison with the nominal composition (values in bracket).

Alloy	Ni (at.%)	Mn (at.%)	Ga (at.%)	Co (at.%)
C2	53.15 (51.45)	22.03 (23.03)	22.83 (23.52)	2.00 (2)
C4	51.73 (50.40)	21.77 (22.56)	22.58 (23.04)	3.93 (4)
C6	50.25 (49.35)	21.72 (22.09)	22.06 (22.56)	5.96 (6)
C8	49.81 (48.30)	20.92 (21.62)	21.18 (22.08)	8.10 (8)

Thin disc specimens of Ø5 mm × 0.2 mm were prepared from the homogenized ingots by using an electron discharge machine (EDM), followed by mechanical grinding. Such obtained discs were used for the determination of characteristic temperatures of martensitic transformation and its reverse transformation, including M_s, M_f (the finishing temperature of martensitic transformation), A_s (the starting temperature of the reverse transformation) and A_f (the finishing temperature of the reverse transformation), with a differential scanning calorimeter (DSC, Perkin-Elmer diamond, USA) at heating and cooling rates of 10 K min^{-1}. In order to obtain the yield strength $\sigma_{0.2}(M_s)$, cylindrical specimens of Ø5 mm × 8 mm, for compressive stress–strain measurement, were prepared by slicing the rods with an EDM. The compression experiments were conducted on a thermal simulator (Gleeble 3500, USA) at various temperatures in a range of 70–500 °C (beyond the transformation temperatures) with a temperature interval of 50 °C and a crosshead speed of 1 mm min^{-1}. The $\sigma_{0.2}(M_s)$ was obtained by extrapolation in order to avoid the strain-induced martensitic transformation. The microstructure of the martensite was observed by both optical (Axiovert 200MAT, Carl Zeiss Light microscope) and transmission electronic (Tecnai G2 20, Holland) microscopes.

3. Results and discussion

Gibbs free energy change accompanying with martensitic phase transformation, $\Delta G(T)^{P\to M}_{total}$, can be expressed as [17,18]:

$$\Delta G(T)^{P\to M}_{total} = \Delta G(T)^{P\to M}_{chem} + \Delta G^{P\to M}_{non\text{-}chem} \quad (1)$$

where $\Delta G(T)^{P\to M}_{chem}$ is the chemical free energy change of the transformation that converts the crystal structure of the parent phase to that of the martensite without changing the composition and stabilizes the nucleus of the martensite, and $\Delta G^{P\to M}_{non\text{-}chem}$ is the non-chemical free energy change of the transformation that provides the energy needed for the growth of martensite nucleus. Usually, $\Delta G(T)^{P\to M}_{chem} = 0$ corresponds to the thermodynamic equilibrium temperature of the two phases T_0 (estimated as $T_0 = (M_s + M_f + A_s + A_f)/4$ [19]) and $\Delta G(T)^{P\to M}_{total} = 0$ determines the starting temperature of martensitic transformation M_s. At M_s temperature:

$$-\Delta G(M_s)^{P\to M}_{chem} = \Delta G^{P\to M}_{non\text{-}chem}(M_s) \quad (2)$$

which presents the driving force of martensitic transformation.

According to the crystallography of martensitic transformation [20], shape deformation at M_s temperature is involved in the formation and growth of a nucleus of the martensite, which requires an energy E_s. The martensite plates of the $(Ni_{52.5}Mn_{23.5}Ga_{24})_{100-x}Co_x$ alloys were twined (primary twins) and some of them contained secondary twins (substructure) inside the martensite plate. Typical microstructure of the $(Ni_{52.5}Mn_{23.5}Ga_{24})_{100-x}Co_x$ alloys is shown in Fig. 1; the associated formation energy of twins E_t should be considered as a part of the driving force. In addition, the stored energies of volume change caused by martensite transformation E_v, interface formation between parent and martensitic phases E_i and dislocation formation in the parent phase adjacent to the martensite E_d should also be taken into account in the driving force. Therefore, the driving force of the martensitic phase transformation for the $(Ni_{52.5}Mn_{23.5}Ga_{24})_{100-x}Co_x$ alloys can be estimated as:

$$\Delta G^{P\to M}_{non\text{-}chem}(M_s) = E_s + E_t + E_v + E_i + E_d \quad (3)$$

The shape deformation due to martensitic phase transformation is an invariant plane strain represented by a shearing deformation defined by a shearing stress τ and a shearing angle γ; and therefore, the term E_s can be expressed in the form of $V_M\tau\gamma$ [18] with V_M as the molar volume of the martensite. Under such a shearing stress, the parent phase is yielded and changed to martensite; thus the yielding stress of the parent phase at M_s temperature $\sigma_{0.2}(M_s)$ is used for estimation of the E_s, that is:

$$E_s = \frac{V_M\gamma\sigma_{0.2}(M_s)}{m} \quad (4)$$

with a constant m in the range of 2–3 [18]. As known, there are 8 atoms (two molecules) in a non-modulated unit cell of martensite in Ni_2MnGa-type alloys, therefore, the molar volume of the martensite can be determined from lattice parameters a_M and c_M of the martensite by:

$$V_M = \frac{a_M^2 b_M}{2} \times 6.023 \times 10^{23} \quad (5)$$

And the invariant plane strain angle can be obtained by [21]:

$$\gamma = \arctan\left(\frac{\sqrt{(\eta_1^2 - 1)(1 - \eta_1^2\eta_2^2)}}{\eta_1^2\eta_2}\right) \quad (6)$$

where $\eta_1 = (\sqrt{2}/a_P)a_M$, $\eta_2 = c_M/a_P$ and a_P is the lattice parameter of the parent phase.

As shown in Fig. 1, the martensite plates in the $(Ni_{52.5}Mn_{23.5}Ga_{24})_{100-x}Co_x$ alloys were twined; the area of the twin boundary per mole A can be estimated from the average width d of the martensite plate by:

$$A = \frac{V_M}{d} \quad (7)$$

thus the energy associated with the primary twin boundary is $(V_M/d)\Gamma_t$ and Γ_t is the twin boundary energy per area. It is also noted that secondary twins were rarely observed inside some of the

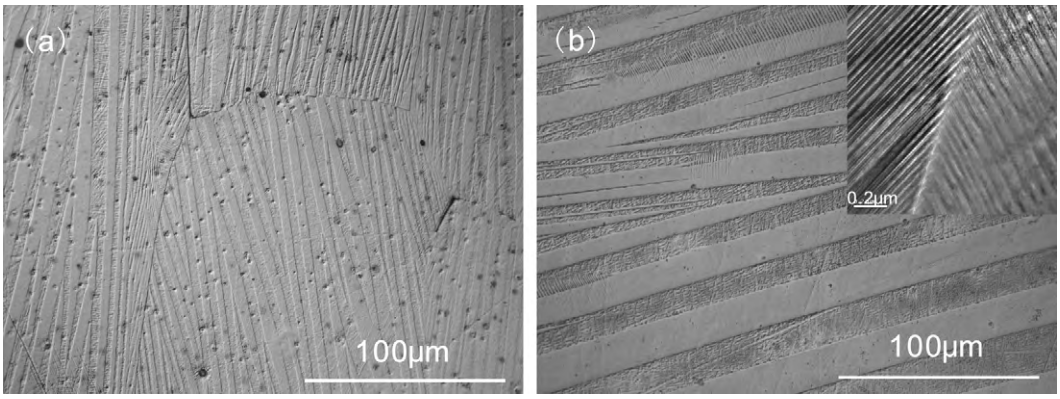

Fig. 1. The microstructures of the martensite in alloys C4 (a) and C8 (b) at room temperature, with typical secondary twins inside the martensite plates shown in the insert.

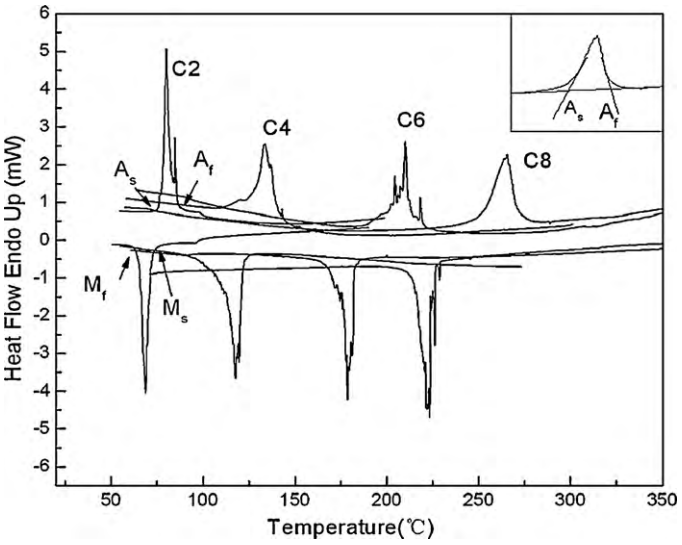

Fig. 2. DSC curves of four alloys, and the insert shows the method of determination of the characteristic transformation temperatures.

martensite plates, the contribution of their boundary energy to the E_t is negligible for the driving force estimation due to its insignificant involvement compared to that of the primary twin boundaries. Therefore, the energy contribution due to the twin boundary of martensite plates is expressed as:

$$E_t = \frac{V_M}{d}\Gamma_t \tag{8}$$

Comparing the lattice parameters of the parent and martensite phases, it is known that the volume change caused by the phase transformation is small; the stored elastic and plastic energies E_v and E_d are unimportant for the driving force of the phase transformation. The $(Ni_{52.5}Mn_{23.5}Ga_{24})_{100-x}Co_x$ alloys are a kind of shape memory alloys, the interface between the martensite and the parent phase is quite movable with low boundary energy that is not counted in the driving force estimation. Based on the above analysis, the expression of the driving force for the martensitic transformation in the $(Ni_{52.5}Mn_{23.5}Ga_{24})_{100-x}Co_x$ alloys can be simplified to:

$$\Delta G^{P\to M}_{non\text{-}chem}(M_s) = \frac{V_M\gamma\sigma_{0.2}(M_s)}{m} + \frac{V_M}{d}\Gamma_t = 6.023\times10^{23}\frac{a_M^2 c_M}{2}\left\{\tan^{-1}\left[\frac{((2a_M^2/a_P^2)-1)^{1/2}(1-(2a_M^2c_M^2/a_P^4))^{1/2}}{2a_M^2c_M/a_P^3}\right]\frac{\sigma_{0.2}(M_s)}{m}+\frac{\Gamma_t}{d}\right\} \tag{9}$$

Fig. 2 shows the DSC curves of the prepared alloys during heating and cooling, from which M_s, M_f, A_s and A_f temperatures were determined. These characteristic transformation temperatures were defined as the temperatures that correspond to the intersection points of the tangent lines to the base line and the peak in the DSC curves, as illustrated by the insert of Fig. 2 with determination of A_s and A_f as the example. The obtained characteristic temperatures of the phase transformations are listed in Table 2. All of the temperatures increased with the increase of Co content in the $(Ni_{52.5}Mn_{23.5}Ga_{24})_{100-x}Co_x$ alloys.

Table 2
Characteristic transformation temperatures of the prepared alloys (°C).

Alloy	A_s	A_f	M_s	M_f	T_0	ΔT
C2	76.9	83.4	72.6	65.1	74.5	1.9
C4	129.4	141.6	122.1	114.9	127.0	4.9
C6	200.1	214.2	182.8	171.4	192.1	9.3
C8	255.1	270.7	224.2	215.7	241.4	17.2

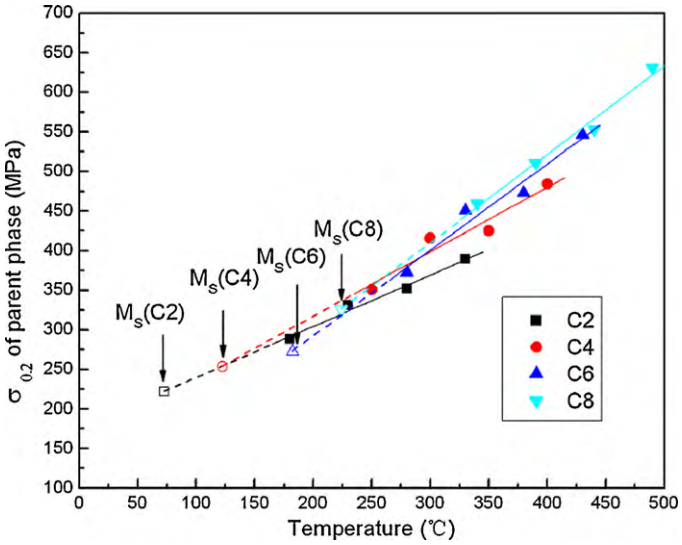

Fig. 3. The yield strength of the parent phase $\sigma_{0.2}$ of the $(Ni_{52.5}Mn_{23.5}Ga_{24})_{100-x}Co_x$ alloys at various temperatures, and the $\sigma_{0.2}(M_s)$ was obtained by extrapolation following the temperature dependence.

Fig. 3 shows the yield strength $\sigma_{0.2}$ of the parent phase as a function of temperature for all the prepared alloys. Such temperature dependence of yield strength, increasing as temperature rises, is contradicted to that observed in conventional metals and alloys due to the intermetallic nature of the Ni_2MnGa based alloys [22]. The value of $\sigma_{0.2}(M_s)$, listed in Table 3, was obtained by linear extrapolation following the temperature dependence of the yield strength indicated in Fig. 3.

The lattice parameters of the martensitic phase of the $(Ni_{52.5}Mn_{23.5}Ga_{24})_{100-x}Co_x$ alloys were determined by X-ray diffraction [23]; their values, together with the calculated V_M and the measured d, are listed in Table 3. By using all the necessary parameters in Table 3, the driving force for the martensitic transformation of the $(Ni_{52.5}Mn_{23.5}Ga_{24})_{100-x}Co_x$ alloys were calculated using Eq. (9), as listed in Table 3, with 6.74 J/m^2 [24] for Γ_t, 3 for m, and 5.824 Å for the average lattice parameter of the parent phase a_P [23]. Fig. 4 shows the graphic relationship between the driving

Table 3
The lattice parameters of the martensitic and parent phases, the yield strength of the parent phase at M_s $\sigma_{0.2}(M_s)$, the average width of the martensite plate d, the estimated molar volume of the martensite V_M and the calculated driving force $\Delta G^{P\to M}_{non\text{-}chem}$ of martensitic transformation of the prepared alloys.

Alloy	a_M (Å)	c_M (Å)	$\sigma_{0.2}(M_s)$ (MPa)	d (μm)	V_M (cm^3/mol)	$\Delta G^{P\to M}_{non\text{-}chem}$ (J/mol)
C2	3.878	6.493	221.8	7	29.39	265.2
C4	3.859	6.542	253.7	12	29.32	304.6
C6	3.855	6.558	272.5	20	29.33	324.8
C8	3.831	6.582	325.3	26	29.08	388.7

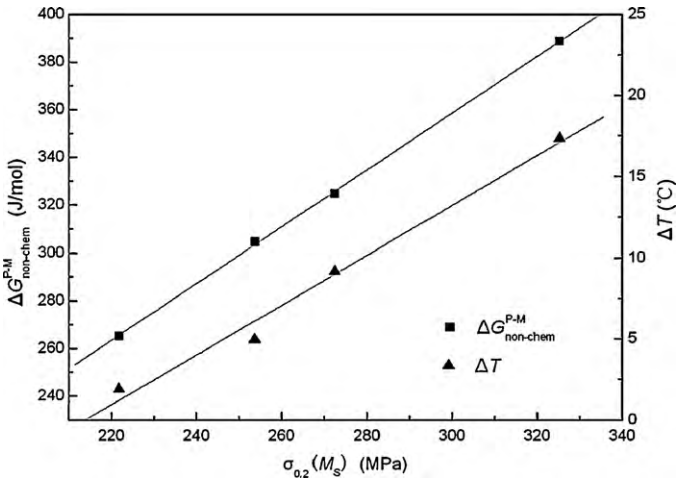

Fig. 4. The driving force for martensitic transformation $\Delta G^{P\to M}_{non\text{-}chem}$ and ΔT of $(Ni_{52.5}Mn_{23.5}Ga_{24})_{100-x}Co_x$ alloys on the yield strength of the parent phase $\sigma_{0.2}(M_s)$.

force and the $\sigma_{0.2}(M_s)$, which can be empirically expressed as:

$$\Delta G^{P\to M}_{non\text{-}chem} = 1.19\sigma_{0.2}(M_s) + 1.63 \quad (10)$$

In previous studies on Fe-based alloys [16,25], the results showed that the M_s decreases with the increase of the $\sigma_{0.2}(M_s)$, which appears to be contradicted to what obtained in the present study (the M_s increases with the increase of the $\sigma_{0.2}(M_s)$). As a matter of fact, it is the $\sigma_{0.2}(M_s)$ that determines the driving force required for martensitic phase transformation, which is also qualitatively measured by the $T(=T_0 - M_s)$; therefore, the dependence of the ΔT on the $\sigma_{0.2}(M_s)$ is more meaningful than that of the M_s temperature on the $\sigma_{0.2}(M_s)$. In the present study, the equilibrium T_0 temperature of the $(Ni_{52.5}Mn_{23.5}Ga_{24})_{100-x}Co_x$ alloys was changed with the added content of Co; however, the ΔT increased with the increase of the $\sigma_{0.2}(M_s)$, as shown in Table 2. In this ΔT point of view, the results from the Fe–C and the $(Ni_{52.5}Mn_{23.5}Ga_{24})_{100-x}Co_x$ alloys are consistent.

4. Summary

The martensitic transformation of $(Ni_{52.5}Mn_{23.5}Ga_{24})_{100-x}Co_x$ alloys was investigated. The characteristic temperatures (M_s, M_f, A_s, A_f) and high temperature yield strength $\sigma_{0.2}(T)$ were experimentally determined, with which the equilibrium temperature T_0 and the yield strength at the M_s temperature $\sigma_{0.2}(M_s)$ for each of the alloy was obtained. The driving force for the martensitic transformation in these alloys were evaluated as $\Delta G^{P\to M}_{non\text{-}chem} = 1.19\sigma_{0.2}(M_s) + 1.63$ according to the equation of $\Delta G^{P\to M}_{non\text{-}chem}(M_s) = ((V_M\gamma\sigma_{0.2}(M_s))/m) + (V_M/d)\Gamma_t$ derived by taking into account the contributions of the shape deformation and twin formation accompanying the martensitic transformation to the energy required to initiate the phase transformation.

Acknowledgements

The DSC characterization was conducted at the Analytical and Testing Center of Huazhong University of Science and Technology. The high temperature yield strength $\sigma_{0.2}$ of the parent phase was measured with a Gleeble 3500 owned by Shanghai Jiao Tong University.

References

[1] A. Sozinov, A.A. Likhachev, N. Lanska, K. Ullakko, Appl. Phys. Lett. 80 (2002) 1746–1748.
[2] Y. Li, Y. Xin, C. Jiang, H. Xu, Scripta Mater. 51 (2004) 849–852.
[3] R.C. O'Handley, S.J. Murray, M. Marioni, H. Nembach, S.M. Allen, J. Appl. Phys. 87 (2000) 4712–4717.
[4] K. Ullakko, J.K. Huang, C. Kantner, R.C. O'Handley, V.V. Kokorin, Appl. Phys. Lett. 69 (1996) 1966–1968.
[5] S.J. Murray, M. Marioni, S.M. Allen, R.C. O'Handley, T.A. Lograsso, Appl. Phys. Lett. 77 (2000) 886–888.
[6] C. Jiang, Y. Muhammad, L. Deng, W. Wu, H. Xu, Acta Mater. 52 (2004) 2779–2785.
[7] N. Okamoto, T. Fukuda, T. Kakeshita, Mater. Sci. Eng. A 481–482 (2008) 306–309.
[8] C. Craciunescu, Y. Kishi, T.A. Lograsso, M. Wuttig, Scripta Mater. 47 (2002) 285–288.
[9] X. Jin, M. Marioni, D. Bono, S.M. Allen, R.C. O'Handley, T.Y. Hsu, J. Appl. Phys. 91 (2002) 8222–8224.
[10] Z.D. Han, D.H. Wang, C.L. Zhang, H.C. Xuan, J.R. Zhang, B.X. Gu, Y.W. Du, Mater. Sci. Eng. B 157 (2009) 40–43.
[11] Z.Y. Gao, G.F. Dong, W. Cai, J.H. Sui, Y. Feng, X.H. Li, J. Alloys Compd. 481 (2009) 44–47.
[12] B. Ingale, R. Gopalan, M. Rajasekhar, S. Ram, J. Alloys Compd. 475 (2009) 276–280.
[13] H.X. Zheng, M.X. Xia, J. Liu, J.G. Li, J. Alloys Compd. 385 (2004) 144–147.
[14] J. Liu, J.G. Li, Scripta Mater. 56 (2007) 109–112.
[15] H.J. Yu, X.D. Jiang, H. Fu, X.T. Zu, J. Alloys Compd. 490 (2010) 326–330.
[16] T.Y. Hsu, J. Li, Z.P. Zeng, Acta Metall. Sin. 22 (1986) A494–A499.
[17] T.Y. Hsu, J. Mater. Sci. 20 (1985) 23–31.
[18] T.Y. Hsu, Acta Metall. Sin. 15 (1979) 329–338.
[19] D.Y. Cong, S. Wang, Y.D. Wang, Y. Ren, L. Zuo, C. Esling, Mater. Sci. Eng. A 473 (2008) 213–218.
[20] C.M. Wayman, Introduction to the Crystallography of Martensitic Transformations, Macmillan, New York, 1964, pp. 67–97.
[21] H. Zheng, Master Degree Thesis, Shanghai Jiao Tong University, Shanghai, 2008.
[22] D. Caillard, Mater. Sci. Eng. A 319–321 (2001) 74–83.
[23] S.M. Yan, PhD Thesis, Huazhong University of Science and Technology, Wuhan, 2010.
[24] J.F. Wan, Y.Q. Fei, J.N. Wang, Acta Phys. Sin. 55 (2006) 2444–2448.
[25] J. Li, T.Y. Hsu, Acta Metall. Sin. 23 (1987) A321–A328.